

Effects on Roll Rate of Mass and Aerodynamic Asymmetries for Ballistic Re-Entry Bodies

LOUIS S. GLOVER*

Applied Physics Laboratory, The Johns Hopkins University, Silver Spring, Md.

"Symmetrical" ballistic-type re-entry bodies have been observed to exhibit erratic roll behavior during flight. This unpredicted behavior can have adverse effects on performance by producing excessive loads and dispersion. To explain the observed phenomena, roll characteristics produced by several types of mass and aerodynamic asymmetries were determined by numerical solution of the equations of motion and by a simplified analytical solution. The asymmetries considered included lateral displacement of the center of gravity and center of pressure, inclination of the principal longitudinal axis to the body geometrical centerline, unequal pitch and yaw moment of inertia about the principal axes, and asymmetric aerodynamic moments. All types of asymmetries, except for the inclination of the principal axis, produced significant roll torque, and various combinations of these asymmetries produced roll-rate histories similar to those observed on flight records.

Nomenclature

B, D, E, G	= functions defined by Eqs. (12, 14, 13, and 11), respectively
c.g.	= center of gravity
c.p.	= center of pressure
C_A	= axial force coefficient = $-F_{X_B}/q_0 S$
C_{m_0}	= asymmetric moment coefficient about the Y_B axis
C_N	= normal force coefficient = $F/q_0 S$
C_{n_0}	= asymmetric moment coefficient about the Z_B axis
d	= reference diameter for aerodynamic coefficients, ft
F	= force; without subscript refers to resultant force normal to the body centerline, lb
F_α	= F/α , lb/rad
g_X	= acceleration along the X_B axis, g 's
I	= moment of inertia; without subscript refers to either I_Y or I_Z , slug-ft ²
l, m, n	= aerodynamic moments about the X, Y, Z axes, ft-lb
M	= body mass, slugs
M_p	= roll damping moment per unit rotational velocity about the X axis, ft-lb-sec/rad
M_q	= pitch (or yaw) damping moment per unit rotational velocity about the Y (or Z) axis, ft-lb-sec/rad
p, q, r	= angular rates about the X, Y, Z axes, rad/sec
$\dot{p}, \dot{q}, \dot{r}$	= angular accelerations about the X, Y, Z axes, rad/sec ²
q_0	= dynamic pressure = $\rho V^2/2$, lb/ft ²
R	= resultant lateral body rate = $(q^2 + r^2)^{1/2}$, rad/sec
S	= reference area for aerodynamic coefficients, ft ²
t	= time, sec
V	= velocity, fps
W	= body weight, lb
X, Y, Z	= principal axes (see Fig. 1)
x, y	= locations in the $X_B Y_B$ plane, ft
$\Delta x, \Delta y$	= dimensions defined in Fig. 2a, ft
α	= angle of attack, rad or deg
δ, ϵ, θ	= angles defined in Figs. 1 and 2, rad
ψ	= direction of lateral force vector (see Fig. 2b), deg
$\Delta\psi$	= $\psi - \psi_0$, deg

ρ	= air density, slugs/ft ³
ω	= undamped aerodynamic pitch (or yaw) frequency = $(F_\alpha \Delta x / I)^{1/2}$, rad/sec

Subscripts

B	= body axis
e	= roll equilibrium conditions
i	= initial conditions at re-entry
0	= conditions at $p = 0$
X, Y, Z	= principal axes X, Y, Z

In the text, boldface type indicates a vector quantity. In the illustrations, vector quantities are indicated by symbols with arrows above them.

Introduction

SYMMETRICAL ballistic-type re-entry bodies have been observed to exhibit roll rates that steadily increase or decrease during flight and, on some flights, change sign several times. Such unpredicted behavior can have adverse effects on performance by producing loads that exceed design limits of the structure or payload if very large roll rates are developed or if the roll rate is driven to roll yaw resonance conditions. On the other hand, large miss distances can result if the roll rate is at resonance or is reduced to nearly zero for an extended period of time.

Therefore, a study of various effects producing roll torque was undertaken to evaluate the importance of each effect.

Discussion

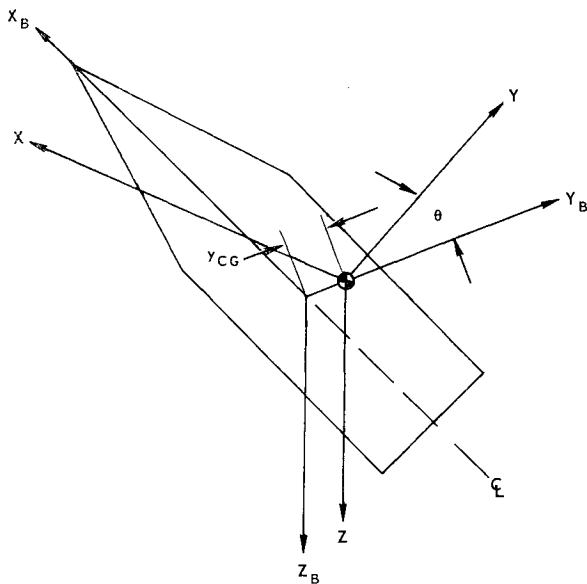
Two sources of roll torque are roll damping and various types of mass and aerodynamic asymmetry. Roll damping results from viscous effects and causes a gradual reduction in roll rate. Although the roll torque produced may be significant, roll damping effects do not explain the observed roll characteristics and effort was concentrated on the effects of asymmetry. The following types of asymmetry were considered (see Figs. 1 and 2).

1) Mass Asymmetry: a) unequal pitch and yaw moments of inertia ($I_Y \neq I_Z$), b) inclination of the principal X axis to the body geometrical centerline (θ), and c) lateral displacement of the center of gravity from the body centerline ($y_{c.g.}$).

2) Aerodynamic Asymmetry: a) asymmetric couple about the Y and Z axes (C_{m_0} C_{n_0}) and b) lateral displacement of the center of pressure from the body centerline ($y_{c.p.}$).

Received June 8, 1964; revision received November 5, 1964. This work was sponsored by the Bureau of Naval Weapons, Special Projects Office, SP-20. The author gratefully acknowledges the contributions of L. L. Cronvich for many suggestions regarding this study and its presentation, of B. F. Fuess and M. P. Guthrie for their assistance with the numerical solutions, and of H. S. Kanely for the preparation of the manuscript.

* Aerodynamics Project Engineer. Member AIAA.



NOTES:

1. AXES X AND Y ARE IN THE $X_B Y_B$ PLANE
2. POSITIVE y_{CG} AND θ ARE SHOWN
3. VELOCITY AND FORCE VECTORS ARE POSITIVE WHEN DIRECTED TOWARD POSITIVE X, Y, OR Z; BODY RATE IS POSITIVE FOR CLOCKWISE ROTATION ABOUT X, Y, OR Z FOR AN OBSERVER FACING THE POSITIVE DIRECTION OF THE AXIS.

Fig. 1 Axis systems.

The problem was simplified by limiting θ and the displacement asymmetries to the XY plane. The center of pressure was assumed to lie on a "center of pressure line," which may be inclined (ϵ) to the body centerline.

Using principal axes that roll with the body, the rotational motion about the X, Y, and Z axes is defined by the following equations:

$$\dot{p}I_X = l + (I_Y - I_Z)qr \quad (1)$$

$$\dot{q}I_Y = m + (I_Z - I_X)pr \quad (2)$$

$$\dot{r}I_Z = n + (I_X - I_Y)pq \quad (3)$$

For the asymmetries considered, assuming the angles θ and $\delta = \epsilon + \Delta y/\Delta x$ are small and the magnus effects are negligible, the aerodynamic moments l , m , and n are defined by the following equations:

$$l = -F_Z \Delta x (\delta + \theta) - \theta C_{m0} q D S d + M_r p \quad (4)$$

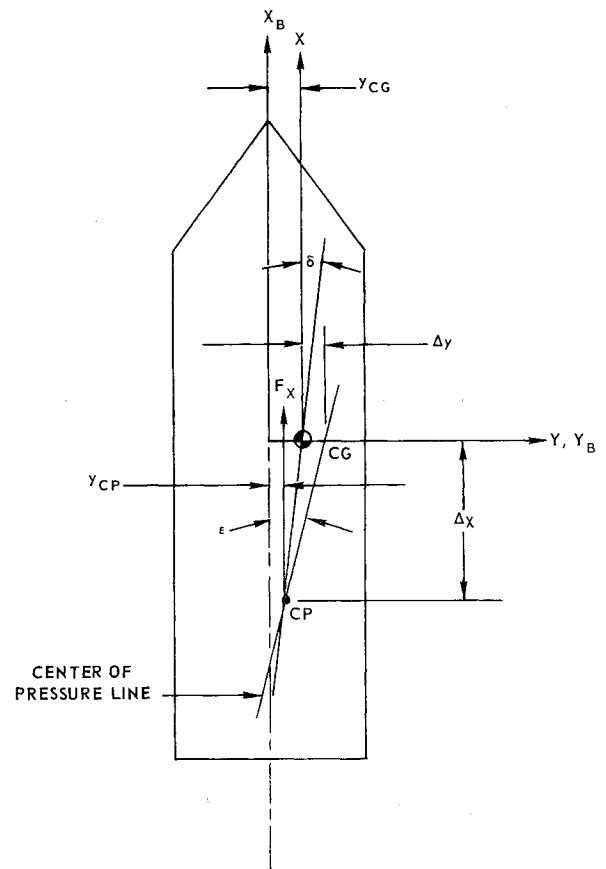
$$m = F_Z \Delta x (1 - \theta \delta) + C_{m0} q D S d + M_q q \quad (5)$$

$$n = F_{X_B} \Delta x \delta - F_{Y_B} \Delta x + C_{n0} q D S d + M_q r \quad (6)$$

These equations, along with equations required to define the aerodynamic force terms, were programed for solution by the IBM 7094 computer. Before considering the results, the general effect of asymmetries will be discussed using approximate solutions to the equations of motion.

Aerodynamic Trim Conditions with $I_Y = I_Z$

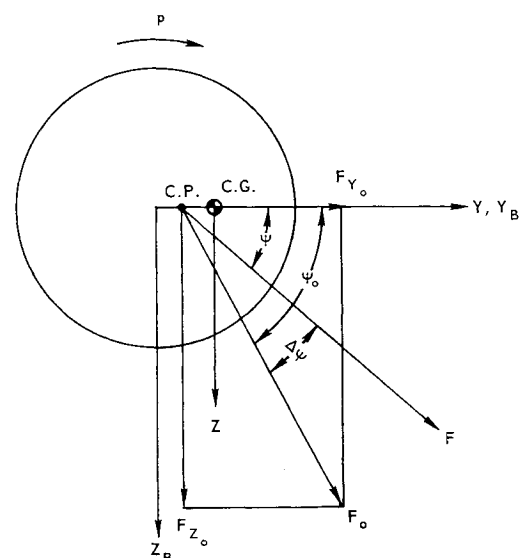
Although a body may re-enter the atmosphere with high initial angle of attack and lateral body rate, the body is in aerodynamic trim about the Y and Z axes during an appreciable portion of the trajectory. For this portion of the trajectory, the solution of the equations of motion may be approximated by simple mathematical expressions.



NOTES:

1. $\theta = 0$ IS SHOWN
2. NEGATIVE Δy IS SHOWN
3. ALL OTHER VALUES ARE POSITIVE

a)



NOTES:

1. NEGATIVE $\Delta \psi$ IS SHOWN
2. ALL OTHER VALUES ARE POSITIVE

b)

Fig. 2 Asymmetry definitions.

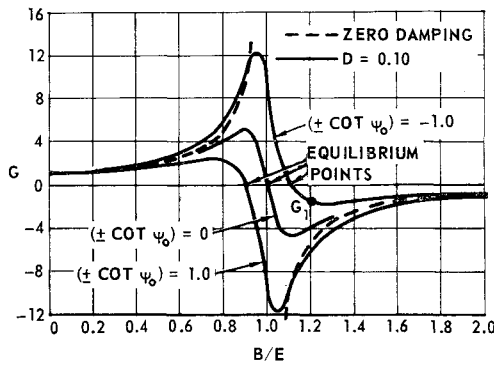


Fig. 3 Typical variations of G with B/E .

For trim conditions, $\dot{q} = \dot{r} = 0$ and the damping terms are negligible. Therefore, for the particular case of zero roll rate and neglecting $\theta\delta$,

$$F_{z0}\Delta x = -C_{m0}q_D S d \quad (7)$$

Substituting into Eq. (4),

$$l = C_{m0}q_D S d \delta \quad (8)$$

Note that the effect of θ on roll torque is small compared to the effect of δ and does not appear in Eq. (8). From Eqs. (1) and (8) and the expression for the dynamic pressure in terms of longitudinal acceleration,

$$\dot{p}_0 = -g_x W d C_{m0} \delta / I_x C_A \quad (9)$$

The effects of roll rate are to modify the magnitude and direction of the trim force and to produce roll damping. The latter effect is neglected in this study. In terms of \dot{p}_0 defined by Eq. (9) and a roll amplification factor G , the roll acceleration may be expressed as

$$\dot{p} = G \dot{p}_0 \quad (10)$$

An expression for the function G , derived¹ using rolling trim conditions defined by Nelson,² is the following:

$$G = \frac{1 - B/E - (\pm D \cot \psi_0)(B/E)^{1/2}}{(1 - B/E)^2 + D^2 B/E} \quad (11)$$

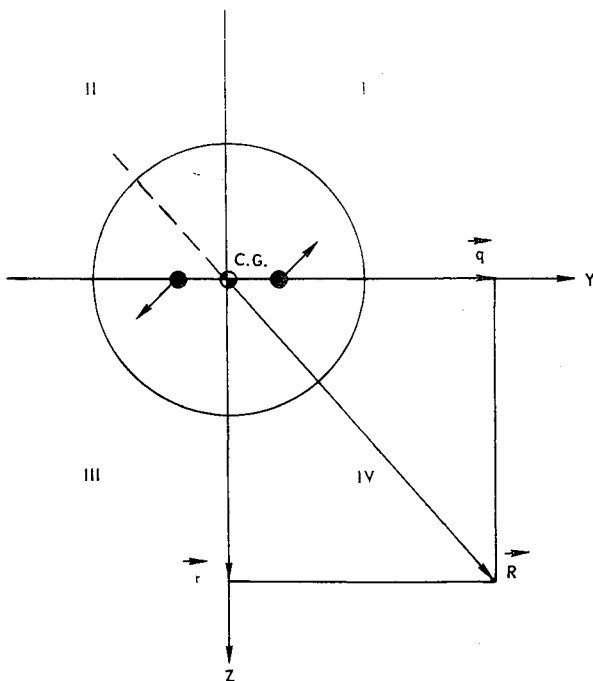


Fig. 4 Roll torque produced by unequal pitch and yaw moments of inertia.

where

$$B = p^2(1 - I_x/I) \quad (12)$$

$$E = \omega^2 - F_\alpha M_q / MVI \quad (13)$$

$$D = \frac{F_\alpha(1 - I_x/I)/MV - M_q/I}{[E(1 - I_x/I)]^{1/2}} \quad (14)$$

$$\cot \psi_0 = (\delta C_A \Delta x / d - C_{n0}) / C_{m0} \quad (15)$$

The \pm sign in Eq. (11) and subsequent equations is to be used as plus for positive roll rates and minus for negative roll rates. It should be noted that the frequency ω is the undamped natural frequency of a nonspinning body having linear aerodynamic characteristics and having planar motion.

Typical variations of G with B/E are shown in Fig. 3. If at some initial time the value of G is negative, such as G_1 , and if \dot{p}_0 and p are of opposite sign, the value of B increases with increasing time. Therefore, unless E increases fast enough to drive G to a positive value, the roll rate will increase without limit. For any other condition, B/E will vary until $G = 0$ where roll equilibrium conditions exist. By setting the numerator of Eq. (11) equal to zero, the value of B/E at roll equilibrium may be expressed as

$$(B/E)_e = \frac{1}{4} \{ [(D \cot \psi_0)^2 + 4]^{1/2} - (\pm D \cot \psi_0) \}^2 \quad (16)$$

For small values of $D \cot \psi_0$

$$(B/E)_e = 1 - (\pm D \cot \psi_0) \quad (17)$$

For the particular case of $C_{m0} = 0$, the roll acceleration is given by

$$\dot{p} = g_x \left(\frac{Wd}{I_x} \right) \left(\frac{\delta^2 \Delta x}{d} - \frac{\delta C_{n0}}{C_A} \right) \left[\frac{(\pm D)(B/E)^{1/2}}{(1 - B/E)^2 + D^2 B/E} \right] \quad (18)$$

These equations were useful for selecting trajectory conditions for the numerical solutions and will be used later to explain the results obtained.

Unequal Pitch and Yaw Moment of Inertia

For a body whose only asymmetry is unequal pitch and yaw moment of inertia about the principal axes, the roll torque is that produced by the term $(I_Y - I_Z)qr$ in Eq. (1). The physical significance of this term for $I_Z > I_Y$ is shown in Fig. 4. The body has mass symmetry except for two small equal masses located on the Y axis equally distant from the c.g. At some instant, the body has a total lateral rotational rate shown by the vector \mathbf{R} . At this time the body rotates about \mathbf{R} and the centrifugal force acting on the two asymmetric

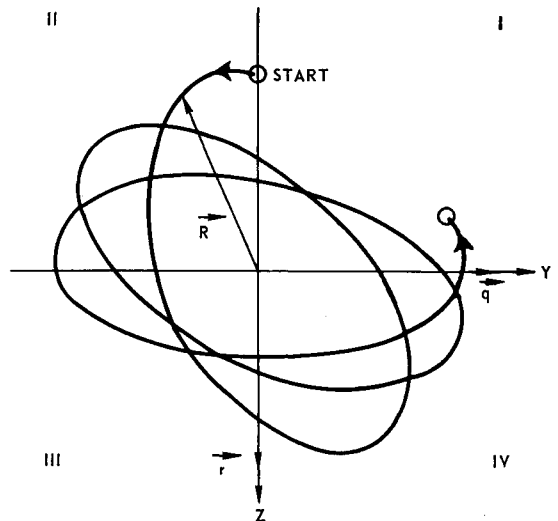


Fig. 5 Typical variation of R with time when aerodynamic forces are significant.

masses produces a couple $(I_Y - I_Z)qr$ about the X axis. The roll torque is positive if \mathbf{R} lies in quadrants I or III and is negative if \mathbf{R} lies in quadrants II or IV.

At very high altitudes, the aerodynamic moments m and n in Eqs. (2) and (3) are negligible and, assuming that a small difference between I_Y and I_Z has negligible effect on \dot{q} and \dot{r} , Eqs. (2) and (3) reduce to the gyroscopic equations of motion. Taking $t = 0$ when r is at a maximum negative value, the solution to Eqs. (2) and (3) is given by

$$q = -R \sin[p_i(1 - I_X/I_Y)t] \quad (19)$$

$$r = -R \cos[p_i(1 - I_X/I_Y)t] \quad (20)$$

Therefore, at $t = 0$, \mathbf{R} lies along the negative Z axis (Fig. 4) and, for positive p_i , rotates counterclockwise at constant amplitude with a frequency $(1 - I_X/I_Y)p_i$. The asymmetric masses and the rotation of \mathbf{R} produce an oscillation in roll rate which has a period $\pi/p_i(1 - I_X/I_Y)$.

The equation for the roll-rate history is obtained by substituting Eqs. (19) and (20) into Eq. (1) and integrating to give

$$p - p_i = \frac{R^2}{2p_i} \left(\frac{I_Y - I_Z}{I_Y - I_X} \right) \frac{I_Y}{I_X} \sin^2 \left[p_i \left(1 - \frac{I_X}{I_Y} \right) t \right] \quad (21)$$

When the vehicle descends to altitudes where the aerodynamic forces are no longer negligible, the body develops a characteristic pattern of motion which depends upon the initial re-entry conditions and the vehicle aerodynamic characteristics.²⁻⁴ The pattern encountered on the trajectories of this study is the slowly rotating elliptical pattern shown in Fig. 5. If $I_Y \neq I_Z$, this type of motion produces an oscillation in roll rate for the same reason discussed previously for the case of zero aerodynamic moments. During the time interval when the major axis lies in quadrants II and IV, a net reduction in roll rate occurs; during the interval when the major axis lies in quadrants I and III, a net increase in roll rate occurs. Therefore, the roll rate oscillates with a period equal to the time required for the axis of the ellipse to rotate 180° . The amplitude of the oscillation increases as the major axis of the ellipse (maximum R) increases and as the rate of rotation of the axis decreases. Therefore, during the portion of the trajectory when the body rates are large, if the elliptical pattern of \mathbf{R} rotates very slowly, large changes in roll rate can occur.

Six-Degree-of-Freedom Solutions

Equations (1-6) and the auxiliary equations required to define body motion during a re-entry trajectory were programed for solution by the IBM 7094 computer. The auxiliary equations used are those given by James⁵ with the following exceptions. Primary interest for this study concerned the high

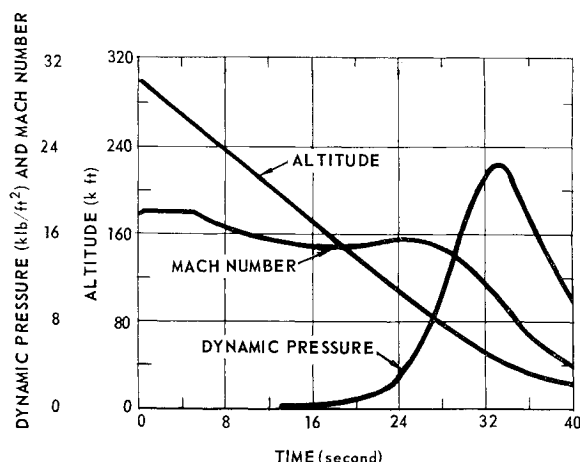


Fig. 6 Trajectory characteristics.

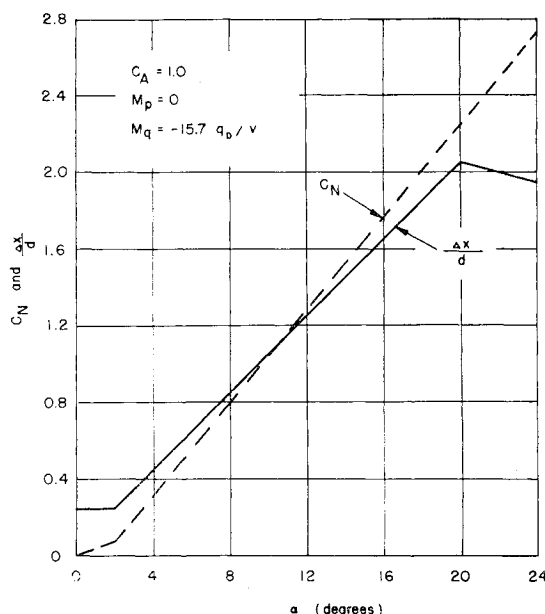


Fig. 7 Aerodynamic characteristics of re-entry body.

Mach number portion of the trajectory. Therefore, the equations were simplified by neglecting the effects of gravity on the flight path angle and by prescribing a dynamic pressure history. This history and the corresponding Mach number and altitude variations based on the 1962 Standard Atmosphere⁶ are shown in Fig. 6.

The ballistic coefficient $W/C_A S$ for the re-entry body of this study is approximately 640, and $I_X/I_Y = 0.10$. The aerodynamic characteristics for the most significant angle of attack region are shown in Fig. 7. Six-degree-of-freedom results are shown for all types of asymmetry considered in this study except for C_{n_0} and θ . These effects were found to be very small and no plotted results are presented.

Combined Mass and Aerodynamic Asymmetries

The roll-rate history for asymmetries $C_{m_0} = 0.010$, $\Delta y/d = 0.00834$, and $\epsilon = +1^\circ$ is shown in Fig. 8. For this trajectory, the initial angle of attack is zero. From the equations based on trim conditions, since p and $\cot \psi_0$ are positive, the G function is typical of that shown for $\pm \cot \psi_0 = 1.0$ in Fig. 3. At re-entry, $B/E \gg 1$ since E is very small and the trim angle of attack remains small as shown in Fig. 9. However, E increases rapidly and, as B/E decreases toward unity, G becomes large and a significant negative roll torque is produced as indicated by Eqs. (9) and (10). The reduction in roll rate and the increase in E drive the vehicle through roll yaw resonance ($B/E = 1$ or $p = 1.05 \omega$ for this body) at $t \approx 21$ sec. The value of B/E continues to decrease and G becomes posi-

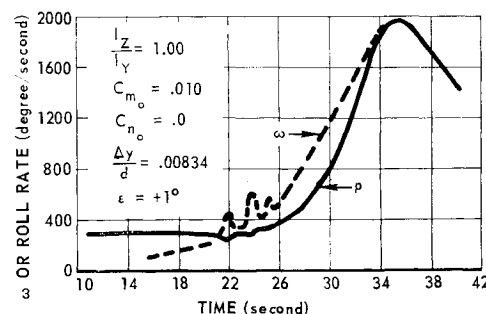


Fig. 8 Roll-rate and aerodynamic-frequency histories for the combination of asymmetries shown: $\alpha_i = 0$, $q_i = 0$, and $r_i = 0$.

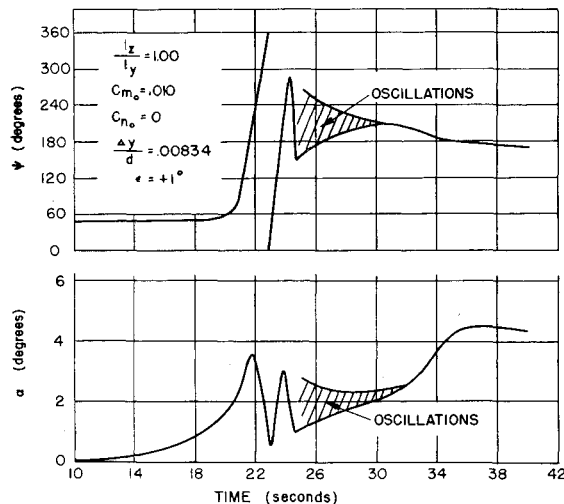


Fig. 9 Angle-of-attack characteristics for the combination of asymmetries shown: $\alpha_i = 0$, $q_i = 0$, and $r_i = 0$.

tive, but the magnitude of \dot{p}_0 and G are so small that the roll torque produced by trim conditions is negligible. However, during resonance, the angle of attack increases to about 3.5° and then oscillates when the resonance condition is passed. This oscillation in α , in conjunction with the asymmetries $\Delta y/d$ and ϵ , produces the small oscillations in roll rate from $t = 21$ to 26 sec. As the vehicle penetrates to lower altitudes, the magnitude of the deceleration increases and a significant roll torque is produced beginning at $t \approx 24$ sec. Since G and \dot{p}_0 are positive, the roll rate increases, seeking the equilibrium condition. For the portion of the trajectory near $t = 34$ sec, $D \approx 0.06$, $\cot \psi_0 \approx 1.74$, and the equilibrium value of B/E from Eq. (17) is 0.893 or $p \approx \omega$. Therefore, the roll rate follows the aerodynamic frequency ω as shown in Fig. 8. The magnitude and direction of angle of attack data given in Fig. 9 are in excellent agreement with those calculated by the trim equations.¹

The roll-rate histories for $C_{m0} = 0.010$ and $\epsilon = -1^\circ$ are shown for several values of $\Delta y/d$ in Fig. 10. The initial angle of attack for these trajectories is 90° . During re-entry, the large angle of attack produces a normal force that acts at some lateral distance from the c.g. This force combined with the roll-rate results in oscillations in the roll rate which persist until $t \approx 30$ sec. For $\Delta y/d = 0$, δ is negative during the entire trajectory, and after about 16 sec G is positive. Therefore, from Eqs. (9) and (10), the roll acceleration is negative and the roll rate steadily decreases as shown in Fig. 10. The roll-rate characteristics from the computer results are in good agreement with results using Eq. (10) which are shown displaced about $50^\circ/\text{sec}$ for clarity in presentation. For $\Delta y/d = 0.0050$ and 0.00834 , δ is negative until $t \approx 30$ sec, but then

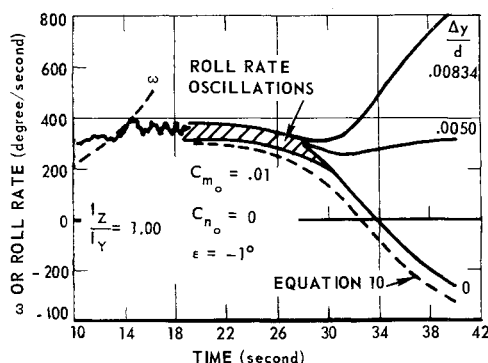


Fig. 10. Roll-rate histories for the combination of asymmetries shown: $\alpha_i = 90^\circ$, $q_i = 0$, and $r_i = 0$.

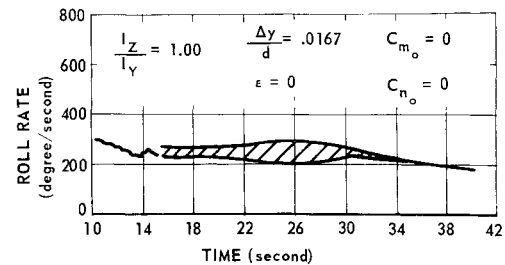


Fig. 11 Roll-rate history for a constant-displacement asymmetry: $\alpha_i = 90^\circ$, $q_i = 0$, and $r_i = 0$.

becomes positive due to the decrease in aerodynamic stability (decrease in Δx) at low angles of attack. This effect produces the reversal in the sign of the roll acceleration at $t \approx 30$ sec. Although not shown in Fig. 10, the magnitudes of the roll accelerations calculated for these values of $\Delta y/d$ by Eq. (10) are also in good agreement with the numerical solutions.

Mass Asymmetry Alone

The roll-rate history produced by $\Delta y/d$ alone is shown in Fig. 11. For the small values of roll rates used for this study, $\Delta y/d$ produces a small roll torque. The value of \dot{p} obtained using Eq. (18) is $-7^\circ/\text{sec}^2$ at $t = 34$ sec, and is in good agreement with the value shown in Fig. 11.

Roll-rate histories for a 2% difference between the pitch and yaw moment of inertia are shown for two values of initial angle of attack in Fig. 12. The amplitude and period of the small roll-rate oscillations near $t = 0$ are properly defined by Eq. (21). However, there are no significant changes in roll rate until $t \approx 20$ sec. By this time the elliptical pattern of \mathbf{R} is well developed. The curve shown in Fig. 5 is the \mathbf{R} trace for the trajectory with $\alpha_i = 135^\circ$ beginning at $t = 22.76$ and ending at $t = 23.36$. This interval corresponds to one-half the period of the roll-rate oscillation for reasons explained previously. Trajectory results show that, from $t = 20$ to 32 sec, the major axis of the \mathbf{R} trace increases to a peak value at $t \approx 23$ sec and then decreases to nearly zero at $t \approx 32$ sec. The axis rotates counterclockwise at $t \approx 20$ sec and the rate of rotation steadily decreases, becomes zero at $t \approx 25$ sec, and then the direction of rotation is clockwise until \mathbf{R} becomes zero. The decrease in the level of roll rate occurs during the interval when the rotation of the axis changes direction.

Some trajectories using different initial re-entry conditions and different aerodynamic characteristics did not show the change in direction of the rotation of the axis, and the roll rate at the end of the trajectory was nearly the same as p_i . The parameters significant to this phenomenon have not been isolated. The theory and data of Nelson and Nicolaides²⁻⁴ show that the epicyclic nature of the body motion can produce \mathbf{R} histories similar to those required to produce a change in the roll rate. However, these results were obtained for bodies having mass symmetry and linear aerodynamic characteristics and the reversal in direction of the rotation of the axis occurs at conditions near roll-yaw resonance. The observed phenomenon occurs at conditions far removed from roll-yaw resonance for bodies having unequal I_Y and I_Z and nonlinear aerodynamic characteristics. A trajectory with conditions identical to those used for the $\alpha_i = 135^\circ$ case in Fig. 12, except that the body had mass symmetry, shows an \mathbf{R} trace in which the axis of the ellipse continues to rotate counterclockwise throughout flight. The magnitudes of α_i and \mathbf{R}_i and the nature of the nonlinearity in the aerodynamic characteristics were also found to be important factors in producing this phenomenon. Therefore, the theory of Nelson and Nicolaides is not directly applicable to the analysis of this motion.

Summary

The effects on roll-rate history of the asymmetries considered in this study are summarized as follows:

1) A 2% difference between the pitch and yaw moment of inertia may produce a significant change in roll rate. The effect occurs at a time in the trajectory when the lateral body angular rates are near maximum, and changes in roll rate cease when the lateral rates become damped to small magnitudes. The effect is sensitive to the body lateral rate history and, therefore, to initial re-entry conditions and body aerodynamic characteristics. A six-degree-of-freedom simulation with accurate representation of nonlinear aerodynamic characteristics is required to assess the magnitude of this effect.

2) An inclination of the principal axis to the body axis of 1° produces small oscillations in roll rate when associated with high angle of attack and roll-yaw resonance at high altitude. Otherwise, the effects on roll rate are negligible.

3) A constant lateral displacement of c.g. and c.p., Δy , produces the same effect given previously for item 2. In addition, at lower altitudes where the dynamic pressure is high, a roll torque is produced which always tends to reduce the magnitude of the roll rate. Therefore, the effect is similar to roll damping and the roll equilibrium condition is zero roll rate. This effect can be appreciable when the aerodynamic stability is low or when conditions are near roll-yaw resonance.

4) A lateral displacement of c.g. and c.p., Δy and ϵ , combined with an aerodynamic moment asymmetry C_{m_0} , is very effective in producing a roll torque, except for very large values of roll rate compared to the aerodynamic frequency and for a very narrow band of roll rates near roll yaw resonance. The roll torque may be either positive or negative and roll-rate reversal can be produced. The roll equilibrium condition is very close to the roll yaw resonance condition. The maximum torque tends to occur at maximum dynamic pressure but may be shifted to some other condition if the aerodynamic stability changes markedly during the trajectory.

5) A constant lateral displacement of c.g. and c.p. combined with an aerodynamic moment asymmetry C_{n_0} produces effects similar to those indicated for item 3, except that the roll torque may either increase or decrease the roll rate, depending upon the sign and magnitude of C_{n_0} .

6) Equations (9-18) may be used to assess the effects on roll characteristics of mass and aerodynamic asymmetries for bodies of arbitrary shape, provided that the configuration has static aerodynamic stability. If the aerodynamic characteristics and asymmetries do not change significantly during

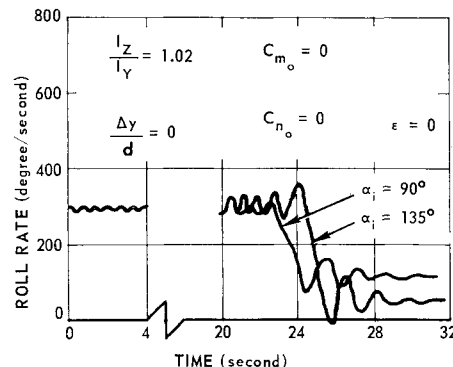


Fig. 12 Roll-rate histories for unequal pitch and yaw moments of inertia: $q_i = 0$, $r_i = -150^\circ/\text{sec}$.

re-entry, and if the roll rate is low compared to the aerodynamic pitch frequency for the major portion of re-entry, then the total change in roll rate from initial re-entry to impact increases with a) increasing initial velocity, b) decreasing magnitude of initial flight path angle, c) increasing magnitude of the asymmetry $\Delta y/d$, d) increasing ballistic coefficient $W/C_A S$, e) decreasing magnitude of the asymmetry coefficient, $I_x/C_{m_0} S d$, and f) decreasing aerodynamic static stability $\Delta x/d$.

References

- 1 Glover, L. S., "Analytical expressions for the effect on roll rate of mass and aerodynamic asymmetries for ballistic-type bodies," The Johns Hopkins University, Applied Physics Lab., TG-560 (March 1964).
- 2 Nelson, R. L., "The motions of rolling symmetrical missiles referred to a body-axis system," NACA TN 3737 (November 1956).
- 3 Nicolaidis, J. D., "On the free flight motion of missiles having slight configurational asymmetries," Ballistic Research Labs., Aberdeen Proving Ground, Rept. 858 (June 1953).
- 4 Nelson, R. L., "Measurement of aerodynamic characteristics of re-entry configurations in free flight at hypersonic and near orbital speeds," Lockheed Missiles and Space Div., TR 6-90-61-37 (July 1961).
- 5 James, R. L., Jr., "A three-dimensional trajectory simulation using six degrees of freedom with arbitrary wind," NASA TN D-641 (March 1961).
- 6 U. S. Standard Atmosphere, 1962 (U. S. Government Printing Office, Washington, D. C., December 1962), pp. 108-147.